HERA; THE ACCELERATOR AND THE PHYSICS*

By B. H. Wiik

II. Institut für Experimentalphysik, Universität Hamburg and Deutsches Elektronen-Synchrotron DESY Hamburg**

(Received August 24, 1984)

Technical description of the electron-proton colliding beam facility HERA is given. The physics programme for this accelerator is outlined.

PACS numbers: 07.77.+p

1. Introduction

In the first part of this report I discuss the electron-proton colliding beam facility HERA and give an update of the status and the machine parameters. The physics programme will be discussed in the second part.

In 1979 a detailed feasibility study [1] of the project was organized by the European Committee on Future Accelerators (ECFA) and this was followed by a technical design report [2] prepared by DESY in collaboration with other institutions. This work resulted in a formal proposal to the German authorities to construct a large electron-proton colliding beam facility designed to collide 820 GeV protons with 30 GeV electrons in four interaction regions. These studies have also been the basis for several [3, 4] workshops. The project was authorized by the German authorities in April of 1984 and actual construction started a month later.

Besides Germany, institutions in Canada, France, Netherlands, Israel, Italy and the United Kingdom have expressed interest in joining the HERA project. The collaboration is modeled after the construction of large experimental facilities; the collaborating institutions contribute machine components to be built in the home countries and manpower.

---

* An updated version of the talk given at the XXIII Cracow School of Theoretical Physics, Zakopane, May 29 — June 12, 1983.

** Address: Deutsches Elektronen-Synchrotron (DESY), Notkestr. 85, 2000 Hamburg 52, West Germany.

2. The accelerator

2.1. Site and buildings

The layout of HERA is shown schematically in Fig. 1 and the main parameters are listed in Table I.

The machine has a fourfold symmetry; four 360 m long straight sections are joined by four arcs with a geometric radius of 779.2 m yielding a total circumference of 6336 m. The tunnel containing the two rings is located some 10–30 m below the surface resulting in a negligible radiation level on the surface. The tunnel intersects the PETRA ring at a depth of 20 m and only short injection paths are needed to connect the two accelerators.

The installations to provide power, cooling and refrigeration for the accelerator will be located on the DESY site and the distribution to the four experimental halls will be either in trenches on the surface or through the tunnel.

A tunnel diameter of 5.2 m is required in the straight sections and the tenders revealed that it is cheaper to make the complete tunnel with an uniform diameter of 5.2 m rather than to reduce the diameter in the arcs to 3.2 m as proposed. Fig. 2 shows a cut through the tunnel in the arc with the proton accelerator mounted on top of the electron machine and with utilities installed.

The counter rotating beams are brought to collision in the middle of the four long straight sections. At each of these locations there will be a large 7 stories deep subterranean

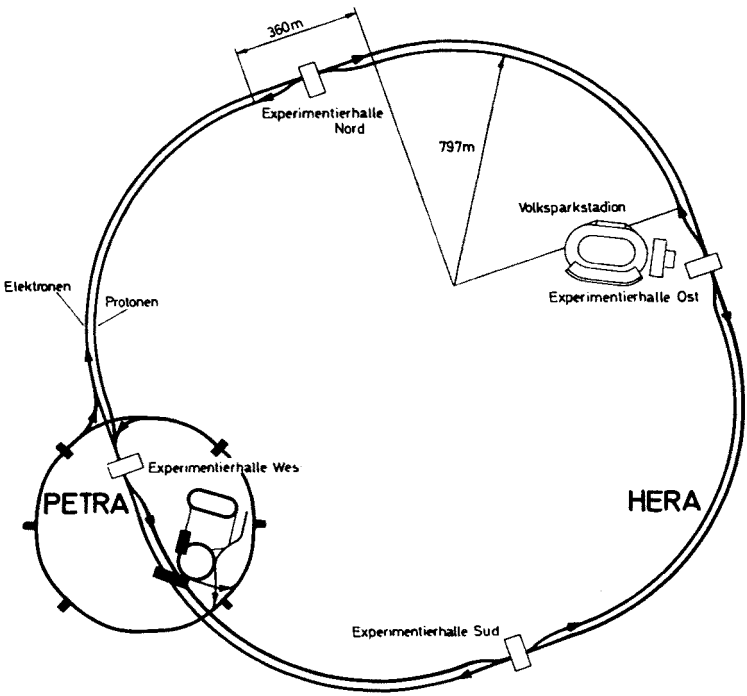

Fig. 1. Schematic layout of HERA

TABLE I

General parameters

	p-ring	e-ring	units
Energy range	820–300	30–10	GeV
Circumference	6336		m
Number of interaction points	4		
Length of each straight section	360		m
Free space for experiments	15		m
Polarization time (30 GeV)	20		min
Magnetic bending field	4.53	0.1849	T
Injection energy	40	14	GeV
RF frequency	499.667	499.667	MHz
Max. circumferential volts	2	290	MV
Circulating current	163	58	m
Number of bunches	210		
Beta functions at interaction points β_x/β_z	3.0/0.3	3.0/0.15	m
Beam size at interaction points	0.12(0.41)/0.027	0.22/0.013	mm
Tune shift $\Delta Q_x/\Delta Q_z$	0.0006/0.0009	0.008/0.014	
Luminosity	0.4×10^{32}		$cm^{-2}\ s^{-1}$
Required refrigeration power at 4.3 K	13/40		kW/(g/s)
Required refrigeration power at 40–80 K	40		kW

building containing the detector, control rooms for experiment and machine and all auxilliary equipment. These buildings provide the only access to the tunnel and components weighing up to 40 to can be brought directly into the experimental hall through a loading shaft 9 m × 6 m. The experimental halls are 25 m along the beam direction and 43 m wide (except hall West which is 35 m wide). The crossing point is 4.6 m above the floor and the halls are served by a 40 to crane.

Bids for the tunnel and for the subterranean buildings were received on February 28 and the contract signed on April 24. The tunnel will be drilled in clockwise direction starting from hall South. Hall South and hall West are now being excavated such that the drilling can start early 1985. Installation of machine components can start in April 1986 in the tunnel section linking hall West and hall South. The civil engineering will be completed towards the end of 1987.

2.2. Design parameters

The general parameters are listed in Table I. The maximum energy of the electron beam is determined by the available RF power and the lower energy by the damping time. The electrons will be transversely polarized due to the Sokolov-Ternov effect [5]. The buildup time for the polarization is 20 min at 30 GeV electron energy and it scales as E^{-5}.

The maximum proton energy of 820 GeV is reached using superconducting magnets with an induction of 4.53 T. The proton orbit must be shortened with respect to the electron orbit in order for electrons and protons to remain in phase. The necessity of moving the proton orbit limits the lowest collision energy to about 300 GeV. The lower limit on the

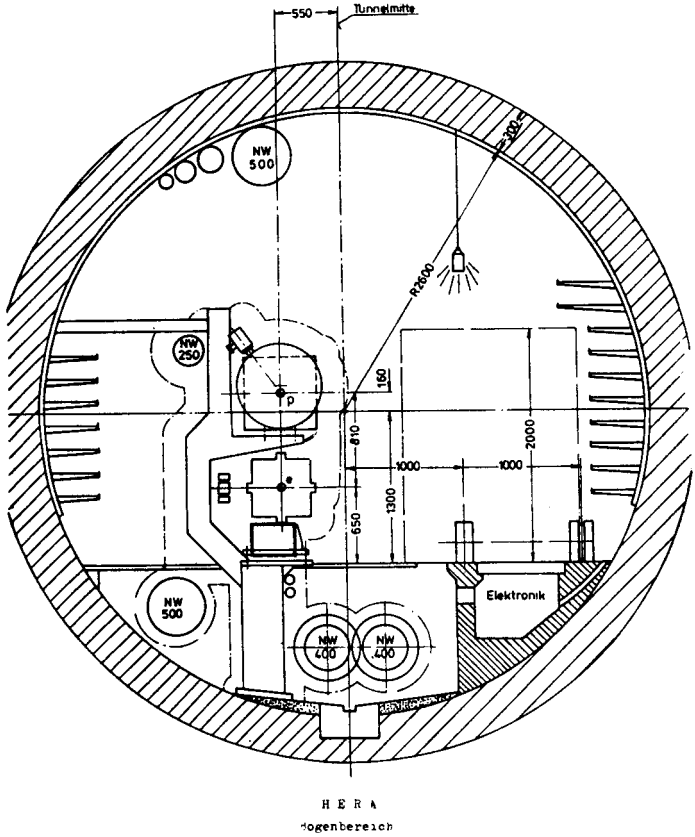

Fig. 2. Cut through the tunnel in the arc

proton injection energy is determined by persistent currents in the superconducting coils. The relative importance of these currents decreases with energy as they cause constant higher multipole fields disturbing the dipole field. We plan to compensate for the average persistent current effects using correction coils wound directly on to the beam pipe. In this case tracking calculations [6] show that a lifetime in excess of 20 hours can be expected at the injection energy of 40 GeV.

In a crossing angle geometry the luminosity is proportional to the proton line density and this favour a high proton RF frequency. In this case the proton RF frequency will be 500 MHz, the frequency used for the DESY electron machine and also foreseen for the electron ring in HERA. In the case of head on collisions the luminosity is nearly independent of the bunch length and a lower frequency of 208 MHz might be favoured. The maximum proton current of 163 mA is divided into 210 bunches spaced 28.8 m apart each containing $1 \cdot 10^{13}$ protons.

The electron ring of HERA will — as a first stage — make use of the large RF system installed at PETRA. Sufficient RF will be left in PETRA to enable the accelerator to reach 14 GeV. The remaining system installed in HERA will enable a current of 16 mA (50 mA)

at 30 GeV (27.5 GeV). The maximum foreseen current of 58 mA in 210 bunches may be reached by either expanding the present system or by installing superconducting cavities. The latter option would lead to substantial saving in power cost.

The filling time of about 20 min for positrons and protons are mainly determined by the estimated 70 s cycle time of PETRA.

2.3. Interaction regions and spin rotators

A finite crossing angle makes it possible to design the two HERA rings without common elements such that the electron and the proton energy might be chosen independently and the synchrotron radiation is minimized by locating bending magnets far away from the interaction region. However, the allowable tune shift has been found to be reduced in a crossing geometry due to synchrotron-betatron resonances [7]. At DORIS the crossing angle leads to a ΔQ-reduction by about a factor of 3. For a proton beam the reduction factor is expected to be even larger [8] since the protons are not damped by synchrotron radiation. An alternative layout for head on collisions is available. At present we favour the head on solution.

The ability to collide electrons (positrons) of well defined helicity with protons provides a very important tool in the investigation of neutral and charged current interactions. This requires that the electron (positron) beam is transversely polarized in the arcs and that the transverse polarization is turned into a state of defined helicity before the collision and that its transverse polarization is restored upon entering the next arc. By empirically compensating [9, 10] those harmonics of the vertical orbit distortions which are close to the number of spin precessions per revolution, transverse polarizations close to the theoretical limit of 92.4% has been achieved [11] routinely with PETRA. High transverse polarizations are therefore expected at HERA since the machines only differ by a factor 1.5 in energy. Furthermore, the depolarization due to beam-beam interactions have been found to be small for the Q values listed above. The spin rotators will also produce depolarizing effects.

An optics solution for a spin rotator [12] employing horizontal and vertical bends has been worked out in detail. About 80% polarization can be reached with this design. To change helicity, magnets must be physically moved and the rotator only works for a limited energy band. An alternative rotator [13] consisting of a large superconducting solenoid and a horizontal bending magnet has also been investigated. At present we favour the solution using vertical and horizontal bending magnets.

2.4. Injection

The booster accelerators are shown schematically in Fig. 1.

PETRA suitable modified [14] serves as the final stage for both electrons (positrons) and protons. The RF system remaining at PETRA limits the electron (positron) energy to 14 GeV. A special beam optic with rather weak focusing of the proton beam will permit acceleration to 40 GeV.

DESY II [15] — which will be used to accelerate single electron (positron) bunches, is a new 9 GeV electron synchrotron under construction in the same tunnel which also

houses the present DESY Synchrotron. DESY II will be completed in March 1985 and will become fully operational in March of 1986.

H^- ions from a new 50 MeV linac [16] are stripped and injected for 10 revolutions into DESY III where they are captured into 11 RF buckets with the final bunch spacing of 28.8 m. The protons are accelerated to 7.5 GeV and transferred in one go to PETRA. The procedure is repeated and the 22 bunches in PETRA are accelerated to 40 GeV. At this energy the protons in PETRA are rotated by 90° in longitudinal phase space and injected into the RF buckets in HERA. During the complete injection cycle the protons never cross transition.

The linac is under construction and will become operational in spring of 1987. The rebuilding of DESY I into DESY III [17] will start after the completion of DESY II. The aim is to inject electrons into the first quadrant in HERA by February 1987 and protons into the first quadrant by April 1988.

2.5. Electron ring components

The dipole, quadrupole and sextupole magnets of the HERA electron ring will be mounted and aligned on a common strong back before being brought into the tunnel. Compared to the proposal the electron half cell length has been increased to 11.769 m. The dipole has a length of 9.1999 m and is excited by a single Cu conductor. Prototypes of the various magnets are now under construction.

The critical energy and the power density of the synchrotron radiative are similar to the values occuring in PETRA and do not represent a problem. It has been proposed to use a Cu-vacuum chamber which would contain most of the synchrotron radiation.

2.6. Proton ring components

For the proton ring superconducting dipole, quadrupole and correction magnets must be developed.

The properties of the bending magnet (warm iron) and the quadrupoles are listed in Table II.

TABLE II

Superconducting magnet parameters

Parameters	Dipole	Quadrupole	Units
Number of magnets	656	304	—
Magnetic length	6.08	1.90	m
Induction	4.53	—	T
Gradient	—	91.2	T/m
Bore	56	56	mm
Nominal current	5582	5582	A
Load factor (4.6 K)	0.89	0.86	—
Stored energy	560	76	kJ
Mass	5750	448	kg

Prototypes of two different bending magnets have been built, a warm iron magnet built at DESY and a cold iron magnet built at Brown-Boveri, Mannheim, in collaboration with DESY. Both magnets are of the cold bore type. A cross section of the two magnet types is shown in Fig. 3a, b.

Of the warm iron type, so far a total of 6×1 m long coils, 3×6 m long full size magnets and 7×6 m long coils have been built and partly tested.

The results [18] can be summarized as follows:

— the tooling is well suited for mass production
— the magnets reach the short sample limit in few training steps
— the field quality is acceptable
— the critical field is about 15% above its nominal value.

The magnets are cooled by one phase helium. At the end of each octant the one phase helium is expanded through a Joule-Thompson valve and the ensuing two phase helium is returned through the magnets in good thermal contact with the one phase helium. The temperature of the magnets is determined by the pressure in the two phase line. The heat shield is maintained between 40 K and 80 K by passing cold helium gas through the outer cryostat.

Three full size cold iron magnets have been ordered from BBC, Mannheim, and the first magnet of this type reached the design value without quenching.

Based on the present experience, we propose to combine some of the advantages of the cold and warm iron magnets into a hybrid magnet [19]. It uses the collared coil developed for the warm iron magnet. The collared coil is nestled directly inside the cold iron. The hybrid magnet has the following characteristic design features:

— passive quench protection using cold or warm diodes
— the iron contributes 22% to the magnetic induction (4.5 T → 5.2 T)
— a simple cryostat with a low heat loss
— the induction increase nearly linearly with the current up to 6.5 T.

Multipoles due to iron saturation are small.

We also propose to increase the magnetic length from 6.08 m to 9.18 m — i.e. a half cell consists of two instead of three bending magnets. The number of magnet interfaces is thus reduced.

The first full size prototypes will be ready early 1985.

Two full size quadrupole [20] magnets have been built and tested at Saclay. They reached the design gradient without quenching and the field quality is acceptable. Two hybrid quadrupoles are now under construction.

The quadrupole and sextupole correction magnets [21] are wound directly on the cold dipole beam pipe. Two 1 m long coils made by NIKHEF and by HOLEC, a Dutch company, have been successfully tested at DESY. The first 6 m long coil is presently being prepared for testing at DESY. A 0.7 m long superferric magnet installed into the quadrupole cryostat, will be used for beam steering. The first prototype of such a magnet has been built by NIKHEF and successfully tested at DESY.

The refrigeration system must provide 13 kW at 4.6 K, 40 g/s of liquid Helium for cooling the leads and 40 kW at 50 K. In the proposal refrigerators were installed in each

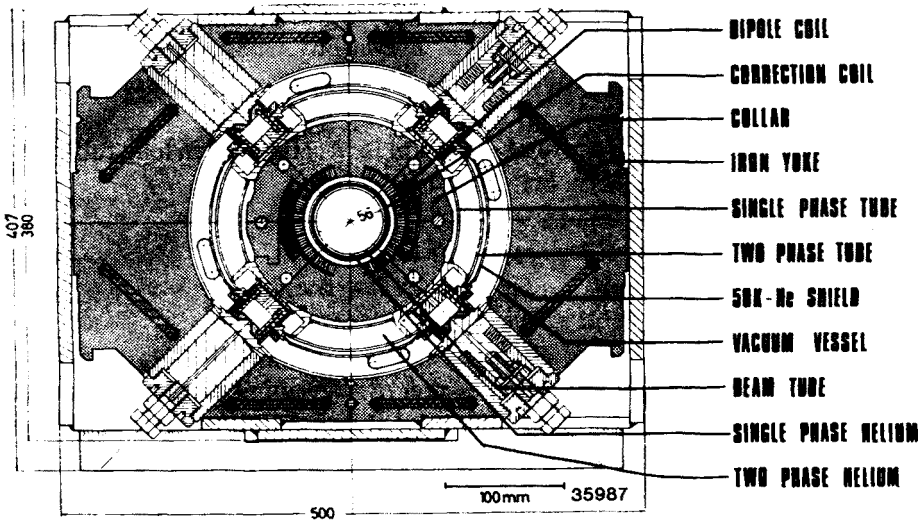

Fig. 3a. Cross section of the warm iron magnet

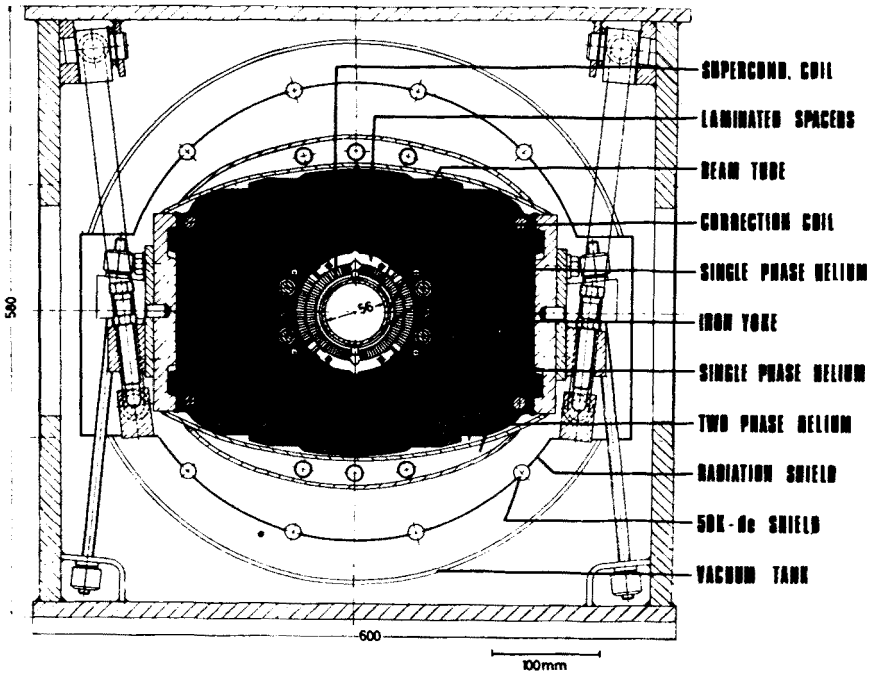

Fig. 3b. Cross section of the cold iron magnet

experimental hall cooling adjacent octants, with a centrally located compressor station. We now propose [22] to also locate the refrigerators centrally and to pipe liquid helium to the four experimental halls where it is distributed to the octants. The refrigeration load listed above is divided on two refrigerators each providing 50% of the load. Full redundancy can be achieved by installing a third refrigerator.

3. Electron-proton interactions at high energies

3.1. Introduction

It has been shown experimentally that the proton contains pointlike constituents (quarks) confined by the strong interaction and that an electron incident on a proton interacts directly with one of these constituents in accordance with Fig. 4. The interaction between a lepton and a quark is mediated by a neutral or a charged spacelike current. The variables and the kinematic of the process is defined in Fig. 4.

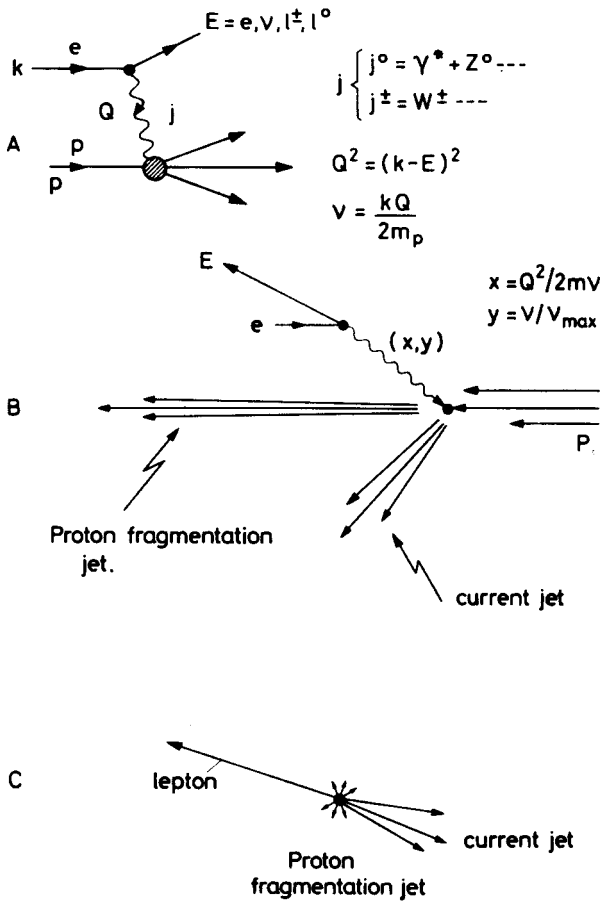

Fig. 4. Kinematic of deep inelastic electron-proton collisions

The physics programme [1, 2, 23, 24] at an ep collider may be summarized as follows:
1) Determine the properties of the spacelike electroweak current at a mass which is large compared to the characteristic mass of the weak interaction. Measurements with electrons and positrons in well defined helicity states can be used to determine the properties of both charged and neutral currents in detail. For example, measurements with left handed positrons or right handed electrons are very sensitive probes for new weak currents.

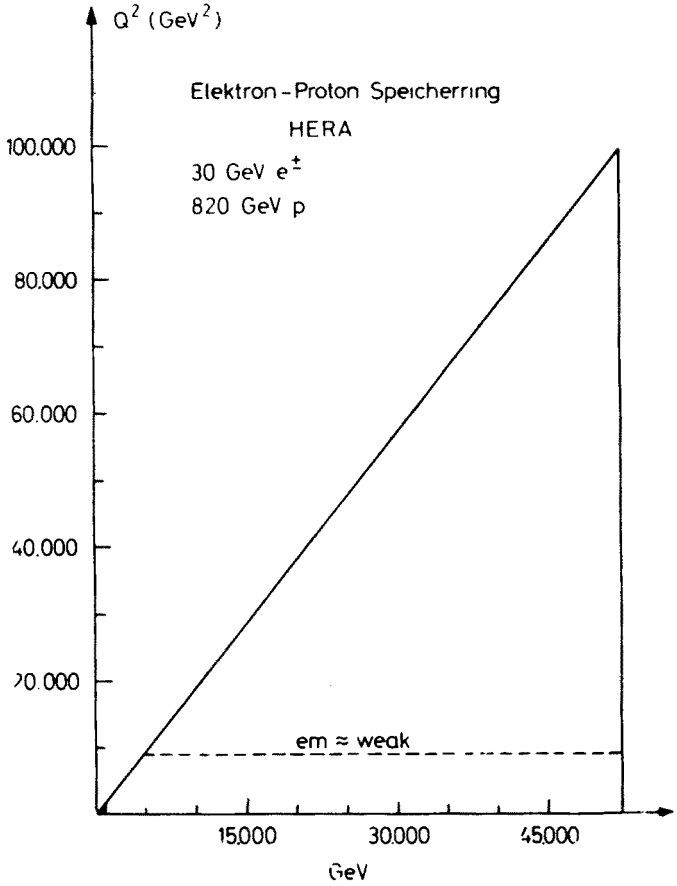

Fig. 5. Kinematical region in Q^2 and ν which can be explored with HERA

2) Use the local, well defined electroweak current to explore the proton at distances down to 10^{-17} cm. Measurements of the structure functions will pose stringent tests of our present understanding of the strong interaction. Such measurements may also reveal new constituents of the proton or they may show that quarks are composite objects.
3) Search for new phenomena. Examples are the search for free quarks, for supersymmetric particles and for elementary particles with combined lepton and baryon numbers, the leptoquarks.

This programme demands a large kinematical area. The kinematical region available with HERA is shown in Fig. 5. The scale is set by the black dot in the left hand corner representing the region which can be explored using a 1 TeV muon or neutrino beam on a fixed target. It is clear that HERA opens a new kinematical region well outside that available with present or planned fixed target machines.

The Q^2-value corresponding to the characteristic mass of the weak interaction squared is shown as the dotted line. A large kinematical region is available beyond this Q^2 value.

The final state topology in deep inelastic electron-proton interactions is striking and easy to recognize. As indicated in Fig. 4b and 4c the scattered lepton appears at a large angle with respect to the beam axis and the corresponding transverse momentum is balanced by the struck quark which fragments into a jet of hadrons appearing at large angles on the opposite side of the beam axis. The remains of the proton give rise to a forward jet of hadrons focused along the proton beam axis with no net transverse momentum. Because of the imbalance between incident electron and proton momenta the particles will in general emerge in the forward hemisphere along the proton direction. The proton jet, the quark jet and the lepton defines a plane with small momenta transverse to the plane and large momenta in the plane.

Simply on the basis of topology it seems unlikely to confuse a deep inelastic electron--proton event with a background event such that the accessible Q^2-range appears to be limited by rate and not by background. Note that particles from the lepton vertex and the quark vertex are kinematically well separated. In the standard model only a single neutrino or a single electron are allowed at the lepton vertex. The observation of any other type of particles or of jets emerging from the lepton vertex is a unique signature of new physics.

The Q^2-range which can be explored depends therefore only on the rate which in turn is determined by the luminosity and the center-of-mass energy. To produce 100 charged current events with $Q^2 > 10000\ \mathrm{GeV}^2$ per year requires a luminosity of $1.5 \times 10^{30}\ \mathrm{cm}^{-2}\ \mathrm{s}^{-1}$ — a factor of 40 below the HERA design luminosity. For a luminosity of $10^{32}\ \mathrm{cm}^{-2}\ \mathrm{s}^{-1}$ we expect 100 events a year with $Q^2 > 35000\ \mathrm{GeV}^2$.

3.2. Low Q^2 physics

The electron beam at HERA is equivalent to a well collimated bremsstrahlungsbeam with an endpoint energy of 52 TeV. The untagged photon-proton luminosity is typically of the order of a few percent of the electron-proton luminosity yielding some 10^7 hadronic events per day.

The photon has a dual character, it may convert into a vector meson and interact like a hadron. However, it has also a pointlike part and may induce hard processes like deep inelastic Compton scattering and the QCD analogues of Compton scattering and Bethe--Heitler processes. Note that the QCD Bethe-Heitler process can be used to measure the gluon structure function ($q = u, d, s$) as a function of Q^2 and ν and to search for heavy quarks. A total of 10^5 $c\bar{c}$ pairs are expected to be produced per day at HERA via the QCD Bethe-Heitler process and some 20 $t\bar{t}$ pairs if $m_t = 50$ GeV.

3.3. Properties of the currents

3.3.1. Charged currents

The x, y distribution of charged current events in bins of $dxdy = (0.2)^2$ expected after one month of data taking with an unpolarised 30 GeV electron beam colliding with a proton beam of 820 GeV is shown in Fig. 6. The rates were estimated in the standard model [25] with $m_W = 78$ GeV and form factors parametrized according to Buras and Gaemers [26] and assuming a luminosity of 10^{32} cm^{-2} s^{-1}. Given the distinct signature of charged current events it seems possible to explore a large fraction of the kinematical region.

The expected number of events will be modified as a function of Q^2 by the presence of a heavier vector boson. A heavy vector boson can be observed at HERA provided its coupling constant $g = g_{W\pm}$ and its mass is below 500 GeV.

Right handed currents do not occur in the standard model. Sensitive searches for these currents may be carried out using right handed electrons and left handed positrons. Such measurements will reveal the existence of right handed currents if the mass of the propagator is less than 600 GeV and the longitudinal beam polarisation is at least 80% known to an accuracy of 1%. This mass limit is valid even if the electron is partnered with a massive neutrino L_0 in a right handed doublet.

It is then natural to assume that also the light quarks u and d are partnered with heavy quarks in right handed doublets. The production rate for $e+q \to L^0+Q$ has been

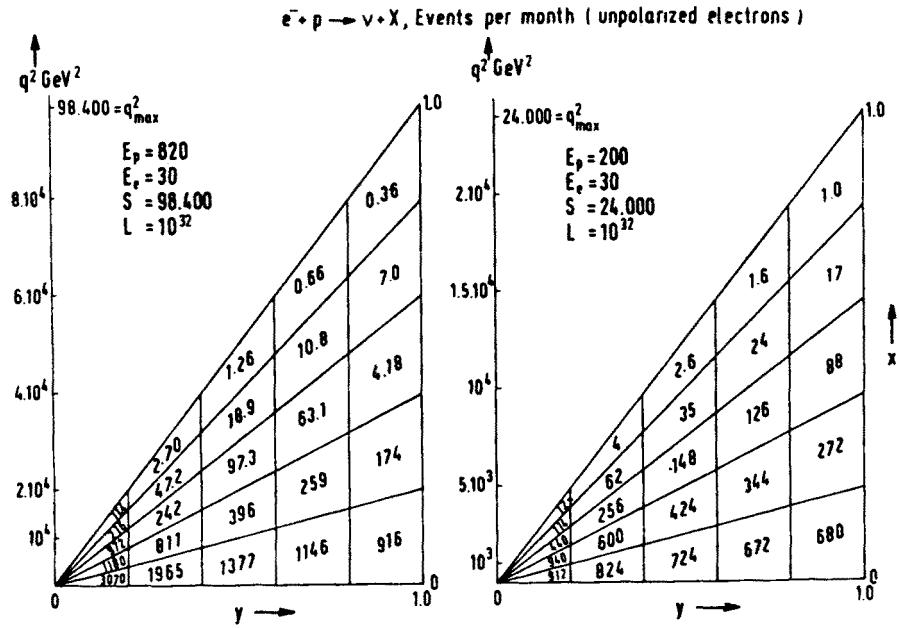

Fig. 6. Number of charged current events in bins of $dxdy = (0.2)^2$ produced per month of data taking assuming of standard model and a luminosity of 10^{32} cm^{-2} s^{-1}. To obtain the number of events expected per year of data taking at the nominal HERA luminosity using left handed electrons multiply the left plot with a factor 8 and the right-hand plot with a factor 5

evaluated with the assumptions listed above plus the assumption that the new current couples with the same strength as the old one. The rates are plotted in Fig. 7 as a function of the heavy quark mass and the mass of the neutral lepton as a parameter.

Leptons and quarks with masses as heavy as 150–200 GeV can be found in this way. The decay of the massive lepton leads to a spectacular signature; the single lepton emerging from the lepton vertex in the standard model will be replaced by $L^0 \to e^- Qq$ — i.e. a high multiplicity jet containing leptons.

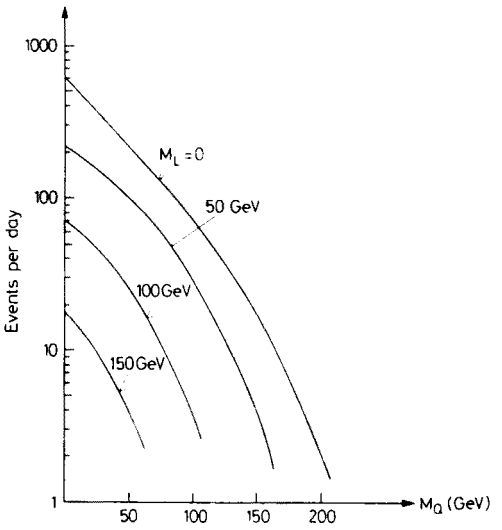

Fig. 7. Number of events per day for $e^- + p \to L^0 + Q + x$ at $s = 9.6 \times 10^4$ GeV^2 assuming left-handed coupling, unpolarised electrons, $m_W = 78$ GeV, Buras-Gaemers parametrization with $\Lambda = 0.5$ GeV and a luminosity of 10^{32} cm^{-2} s^{-1}

Similar remarks can also be made for heavy lepton production via the neutral current.

At $x > 0.4$ only the valence quarks contribute to the cross section — i.e. $e^- + u \to d + x$ and $e^+ + d \to u + x$ are the dominant processes. This makes it possible to study the fragmentation of a quark with a well defined flavour and it also opens the possibility of measuring the Kobayashi-Maskawa mixing angles directly via the process

$$e^- + u \to s + x \quad \text{and} \quad e^- + u \to b + x,$$

$$e^+ + d \to c + x \quad \text{and} \quad e^+ + d \to t + x.$$

3.3.2. Neutral currents

One photon exchange and Z^0 exchange contribute coherently to $e + p \to e' + x$ and both contributions are of similar strength at HERA energies. Measurements of this process can therefore decide if indeed the electromagnetic and weak interactions are manifestations of a single force and if this unification occurs as conjectured in the standard model or if a more complicated mechanism involving several neutral vector bosons is realized

in nature. The number of neutral current events produced per day in a bin $dxdy = (0.2)^2$ is plotted in Fig. 8. Again due to the characteristic topology of deep inelastic events HERA can extend the Q^2 range from the present few hundred GeV^2 out to some 30000–40000 GeV^2.

The presence of a weak current in the amplitude has clear signatures:

1) Parity violation

$$(e_L^- + p \to e^{-'} + x) \neq (e_R^- + p \to e^{-'} + x),$$

$$(e_L^+ + p \to e^{*'} + x) \neq (e_R^+ + p \to e^{+'} + x).$$

This effect can only be caused by a neutral weak current.

2) Appearant C-violation

$$(e_L^- + p \to e^{-'} + x) \neq (e_L^+ + p \to e^{+'} + x),$$

$$(e_R^- + p \to e^{-'} + x) \neq (e_R^+ + p \to e^{+'} + x).$$

Two-photon exchange will also give rise to a charge asymmetry. This effect, however, is expected to be of order $\alpha/\pi \ln(Q^2/m^2)$ with $m \sim 300$ MeV. At large values of Q^2 this effect is small compared to the charge asymmetry caused by Z^0 exchange and it has a different Q^2 dependence.

3) The presence of a $1-(1-y)^2$ term which is not allowed in the one photon exchange approximation. This effect cannot be caused by two photon exchange.

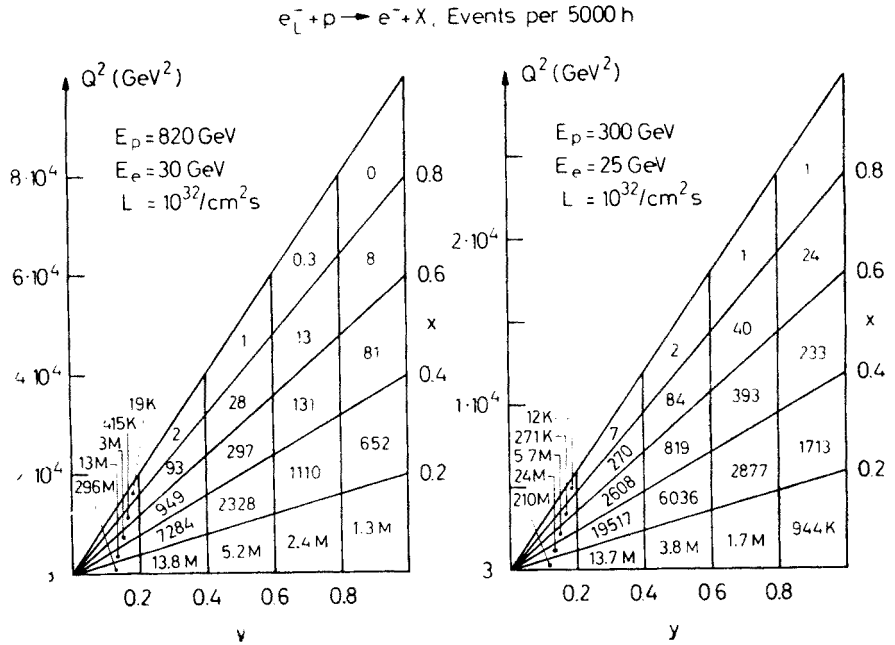

Fig. 8. Number of events per 5000 hrs for $e^- + p \to e^- + x$ at $s = 9.6 \cdot 10^4$ GeV^2 and $s = 3 \cdot 10^4$ GeV^2 and the standard assumptions

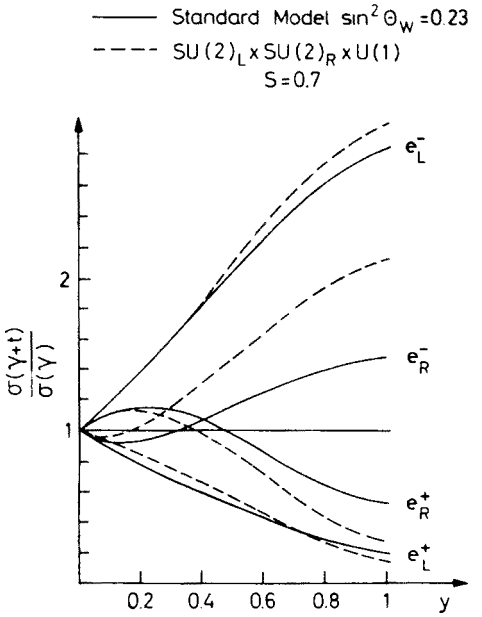

Fig. 9. The ratio $\sigma(\gamma+Z^0)/\sigma(\gamma)$ plotted versus y for $x = 0.25$. The ratio is evaluated for two different weak interaction models

The size of these effects in the standard model is shown in Fig. 9 where the ratio

$$\frac{\sigma(\gamma+Z^0)}{\sigma(\gamma)}$$

evaluated for left and right handed electrons and positrons is plotted as a solid line versus y for $x = 0.25$.

The experiment is sensitive to new neutral vector bosons with mass below 500 GeV.

Flavour changing neutral currents like $e^- + d \rightarrow \tau^- + b$ may appear. In the example above the decay products will emerge on the lepton side instead of a single lepton. Such events would be spectacular and easy to observe.

3.4. Exploring the proton

The resolving power of a spacelike electroweak current increases with $\sqrt{Q^2}$ such that the proton may be probed at shorter and shorter distances with increasing values of Q^2. Measurements at increasing values of Q^2 showed that the form factors are enhanced at low and depleted at high values of x. This observation is naturally explained in any field theory of strong interactions.

The Q^2 evolution of the form factors can be unambiguously computed in Quantum Chromodynamics [27]. Careful measurements of the cross section over a wide range in Q^2 are needed to distinguish the logarithmic scaling violations inherent in QCD from a power series as would occur in a fixed point field theory. Measurements over the entire

kinematical range will be used to confirm or reject the predicted logarithmic Q^2 dependence of α_s.

The correction factor needed to extract the cross section from the raw data are small such that the form factors can be measured with the required relative precision of a few percent over nearly the entire kinematical region.

The slow variation of the form factors with Q^2, as predicted in QCD makes it easy to search for new phenomena which may show up as scaling violations.

As an example of a scaling violation we consider the excitation [28] of colour at small distances and fractionally charged quarks resolved into integrally charged quarks of different colours:

$$u \to u_r(e = 1), \quad u_y(e = 1), \quad u_b(e = 0),$$
$$d \to d_r(e = 0), \quad d_y(e = 0), \quad d_b(e = -1).$$

Thus above the threshold for color thaw:

$$(\tfrac{2}{3})^2 u(x) \to \tfrac{1}{3}(1^2+1^2+0^2)u(x) = \tfrac{2}{3}u(x),$$
$$(\tfrac{1}{3})^2 d(x) \to \tfrac{1}{3}(0^2+0^2+1^2)d(x) = \tfrac{1}{3}u(x).$$

Thus in the valence quark approximation the electroproduction cross section would rise by a factor of 1.7. This model also contains charged gluons. The photon may interact with these gluons and contribute to the longitudinal cross section.

3.5. New physics

All the relevant experimental data are described by the standard model using a consistent set of parameter; furthermore its predictions have been strikingly confirmed by the discovery [29] of the vector bosons $W^{\pm}$ and Z^0 at the $p\bar{p}$ collider. Even so the standard model is not complete and it might simply represent the low energy limit of a more fundamental theory. The model does not contain gravity, a large number of free parameters (27) are needed to fit the data and there is a large number of elementary particles. The very different mass scales occuring in the theory poses technical problems. For example: how can the 100 GeV mass scale for the electroweak unification coexist with the 10^{15} GeV mass scale of the grand unification. Several solutions to this problem have been proposed and the different schemes suggest that there might be new physics within the kinematical range of HERA.

- Composite Higgs fields [30]. A new strong interaction — technicolor — with a scale of $(m_w/\sqrt{\alpha}) \sim O(250)$ GeV occurs. The constituents of the Higgs — techniquarks and technileptons are then bound by this new strong interaction.
- If the Higgs field is composite, perhaps also quarks and leptons are made of common building blocks [31], the preons.
- Supersymmetry [32] establishes a connection between fermions and bosons. To preserve the electroweak unification scale the fermion and boson masses should satisfy the condition

$$|m_F^2 - m_B^2| \leqslant O(1)\ \mathrm{TeV}^2.$$

We will now briefly discuss what HERA can contribute to the study of these proposals.

3.5.1. Technicolor

It is generally accepted that the gauge symmetry must be spontaneously broken to give mass to the intermediate vector bosons and to make the theory renormalizable. It has been proposed, as an alternative to the standard Higgs mechanism, that the symmetry breaking arises dynamically from the gauge interactions themselves. In this model a new set of unbroken non-Abelian gauge interactions with a mass scale of the order of 1 TeV is introduced. This interaction gives rise to a complicated spectrum of technicolourless bound states with mass starting around 1 TeV. In addition, the technicolour interaction will result in leptoquarks, fundamental particles with combined lepton and baryon numbers

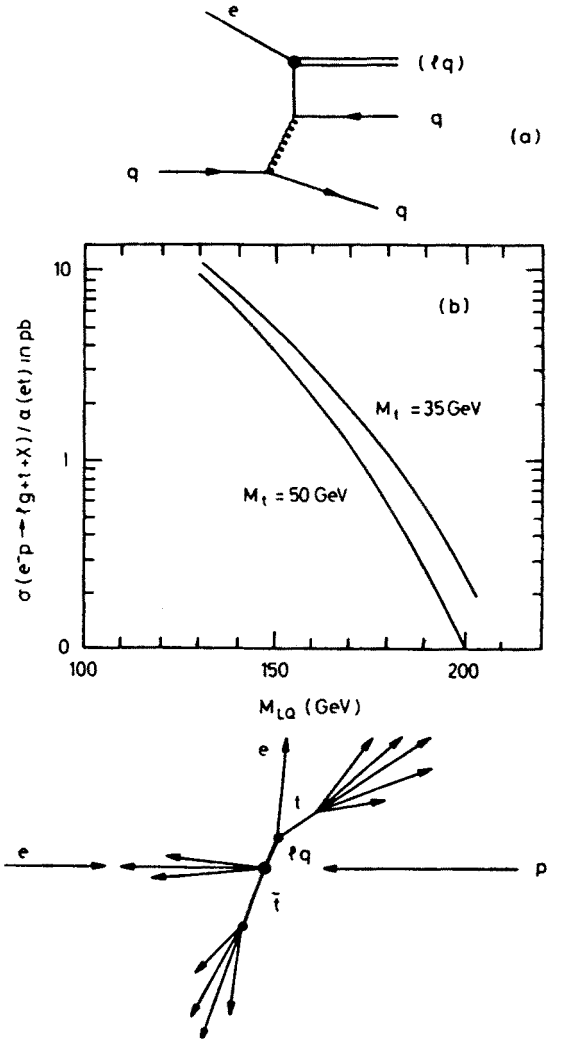

Fig. 10. a) The Feynman graph for producing a leptoquark (lq) in deep inelastic ep reactions; b) The cross section for ep (lq)+x evaluated according to a); c) The final state topology

and a mass predicted around 160 GeV. The cross section for ep → (lq)x resulting from the Feynman graphs in Fig. 10a has been evaluated by Rudaz and Vermaseren [33] and is plotted in Fig. 10b versus the mass of the leptoquark. Roughly one event per day is expected for a leptoquark mass of 160 GeV and a suppression factor $\sin^2 \theta_{et} = 0.05$. The topology of such an event is remarkable with a broad jet, resulting from the decay of the leptoquark (lq) → et, emerging from the lepton vertex.

3.5.2. Composite leptons and quarks

Composite leptons and quarks would lead to an apparent violation of scaling. The cross section would be modified by a form factor

$$F(Q^2) = \frac{1}{(1+Q^2/M^2)}$$

giving rise to scaling violations which are very different from the logarithmic violations expected within QCD. A 10% measurement of the cross section at $Q^2 = 4 \times 10^4$ GeV^2 will be sensitive to $M \leqslant 1$ TeV. Note that the form factors for composite quarks may increase or decrease depending on the charges and the weak coupling constants of the new constituents.

Composite leptons will have excited states and ultimately such leptons will be directly produced. An excited lepton could decay into e+γ, e+Z^0 and e+W leading to peaks in the invariant spectrum. The topology of such final states with several particles emerging from a lepton vertex makes it easy to find.

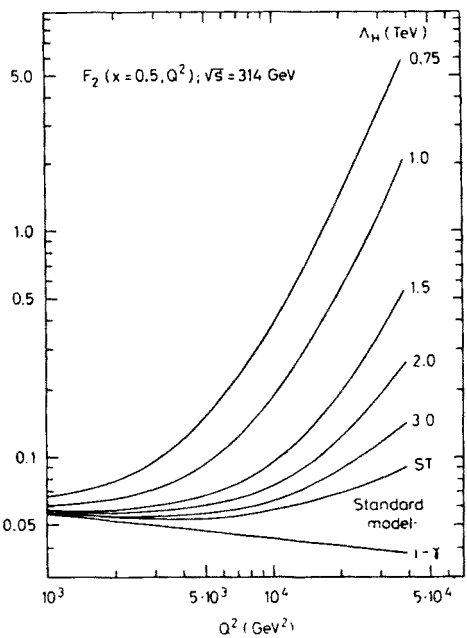

Fig. 11. $F_2(x = 0.5, Q^2)$ is plotted versus Q^2 for ep → e'X. The form factor is evaluated at $\sqrt{s} = 314$ GeV for one photon exchange, for the standard model and for the standard model plus contact interaction

If the quark and the lepton are made of common constituents the normal γ and Z^0 exchange will be modified by contact interactions and the resulting cross section [34] is plotted in Fig. 11. The cross section is increased above the value predicted by the standard model. Using polarized beams HERA is sensitive to values $\Lambda = 1/R_e = 1/R_q = 5$ TeV.

3.5.3. Leptoproduction of supersymmetric particles

Gauging the isospin led to the successful unification of electromagnetic and weak interactions. In supersymmetric theories the same story is repeated for the spin and this leads to a connection between fermions and bosons. Indeed the fundamental feature of supersymmetry is that it can generate fermions from bosons and vice versa. Thus for every particle with spin J there will in principle be two new particles with spin $J \pm 1/2$. A partial list of such new particles is given in Table III.

TABLE III

Possible supersymmetric particles

Types of conventional particles	Spin		
	1	1/2	0
Matter		quark q	scalar quarks $\tilde{q}$
		lepton l	scalar lepton $\tilde{l}$
	$W^{\pm}$	supersymmetric heavy lepton	Higgs scalar
	Z^0	$\tilde{W}^{\pm}$, $\tilde{Z}^0$, H	H
Massless	γ	photino $\tilde{\gamma}$	
		nuinos $\tilde{\nu}$	
	g	gluino $\tilde{g}$	

The presence of scalar quark and spin 1/2 gluons in the proton will strongly affect the form factors at asymptotic values of Q^2. In a conventional QCD 53% of the protons momentum is carried by the quarks as compared to 36% in a supersymmetric world. The problem is that the asymptotic values are approached very slowly for massive supersymmetric particles. Thus it may be difficult to convincingly demonstrate the existence of supersymmetric constituents from the observation of small scaling violations.

However, above threshold scalar quark and scalar leptons can be produced directly via the reactions:

$$e + q \rightarrow \tilde{e} + \tilde{q},$$

$$e + q \rightarrow \tilde{\nu} + \tilde{q}.$$

The observable mass range for supersymmetric particles depends on the signature. If the scalar leptons decay into a jet of particles cross sections are as low as 10^{-38} cm^{-2} corresponding to 10 events a year may be observable. If the dominant decay modes are of the type $\tilde{l} \rightarrow l + G$ and $\tilde{q} \rightarrow q + G$ where G is the undetectable Goldstino, then the background will be more severe. In standard neutral current events, however, the direction and energies

of the scattered lepton and the current jet are strongly correlated. Since in supersymmetric neutral current events the electron and current jet are decay products, this correlation is destroyed and the signal can be enhanced by suitable cuts.

Estimates [35] show that one may produce 500 events a year of the type $e^- + q \to \tilde{e} + \tilde{q}$ with $m_{\tilde{q}} = 100$ GeV, $m_{\tilde{e}} = 40$ GeV, $m_{W_s} = 200$ GeV and $m_B = 60$ GeV. This is easily detectable since the background from the standard neutral current events can be removed by cuts on coplanarity and $y = v/v_{max}$ as evaluated.

Scalar leptons can also be searched for in the process [36] $e + p \to e^* + p \to \tilde{\gamma} + \tilde{e} + p \to e^- + p + 2\tilde{\gamma}$. The signature is very clear with only an electron and a proton in a final state.

4. Time schedule

Some of the most important milestones for the HERA project are listed in Table IV. According to this schedule ep physics will start in 1990.

TABLE IV

MILESTONES

Authorization	April 1984
Start of civil engineering	May 1985
Start installation of machine components	April 1986
DESY II operational	April 1986
Superconducting Magnets, start of series production	July 1986
Electron injection: first quadrant	February 1987
Start commissioning of Proton Linac	April 1987
Delivery of the last magnet for e ring	October 1987
Civil engineering complete	December 1987
Start commissioning of DESY III	December 1987
Refrigeration plant operational	January 1988
Start commisioning of electron ring	March 1988
Proton injection: first quadrant	April 1988
Delivery of last superconducting magnet	October 1988
Start commissioning of proton ring	June 1989
Electron-Proton Physics	early 1990

REFERENCES

[1] Proceedings of the Study of an ep-facility for Europe, U. Amaldi, Editor, DESY 79/48 (1979).

[2] HERA Proposal, DESY HERA 81/10 (1981).

[3] Résumé of the Discussion Meeting *Physics with ep colliders in view of HERA* in Wuppertal, DESY HERA 81/18 (1981).

[4] Proceedings of the Workshop Experimentation at HERA, NIKHEF Amsterdam, June 9–11, 1983, DESY HERA 83/20 (1983).

[5] A. A. Sokolov, J. M. Ternov, *Sov. Phys. Dokl.* **8**, 1203 (1964).

[6] A. Wrulich, DESY HERA 84/07 (1984) and references therein.

[7] A. Piwinski, DESY 77/18 (1972).

[8] A. Piwinski, private communication.

[9] R. Schmidt, DESY M 82-22 (1982).

[10] Résumé of the Workshop *Polarized Electron Acceleration and Storage*, Hamburg, March 1982, DESY M 82-09 (1982).
[11] D. P. Barber, *Polarisation Measurements and Future Plans*, DESY M 83-29 (1983); D. P. Barber et al., *Progress in Measurement and Understanding of Beam Polarisation in Electron Positron Storage Rings*, DESY 83-065 (1983).
[12] K. Steffen, DESY HERA 83/16 (1983) and references therein.
[13] D. P. Barber, J. Kewisch, R. Rosmanith, private communication.
[14] J. R. Maidment, DESY HERA 83/12 (1983).
[15] G. Hemmie, DESY M 82-18 (1982).
[16] Proposal for the HERA Proton Linac, DESY HERA 84/12 (1984).
[17] J. R. Maidment, DESY HERA 83/12 (1983).
[18] G. Horlitz, H. Kaiser, G. Knust, K. H. Mess, P. Schmüser, B. H. Wiik, S. Wolff, DESY HERA 83/21 (1983).
[19] K. Balewski, H. Kaiser, P. Schmüser, private communication.
[20] R. Auzalle, A. Patoux, J. Perot, J. M. Rifflet, DESY HERA 83/27 (1983).
[21] C. Daum, P. Schmüser, DESY HERA 83/02 and 83/07 (1983).
[22] G. Horlitz, DESY HERA 84/02 (1984).
[23] For an early discussion of the physics which can be carried out with a large electron-proton colliding ring see: C. H. Llewellyn-Smith, B. H. Wiik, DESY 77/83 (1977).
[24] CHEEP-An ep facility in the SPS: J. Ellis, B. H. Wiik, K. Hübner, CERN 78-02.
[25] S. L. Glashow, *Nucl. Phys.* **22**, 579 (1961); S. Weinberg, *Phys. Rev. Lett.* **19**, 1267 (1967); A. Salam, Proc. 8th Nobel Symposium, Stockholm Almquist and Wiksells, Stockholm 1968, p. 363.
[26] A. J. Buras, K. J. F. Gaemers, *Nucl. Phys.* **B132**, 249 (1978).
[27] H. Fritzsch, M. Gell-Mann, H. Leutwyler, *Phys. Lett.* **47B**, 365 (1973); D. J. Gross, F. Wilczek, *Phys. Rev. Lett.* **30**, 1343 (1973); H. D. Politzer, *Phys. Rev. Lett.* **30**, 1346 (1973); S. Weinberg, *Phys. Rev. Lett.* **31**, 31 (1973).
[28] J. C. Pati, A. Salam, *Phys. Rev.* **D8**, 1240 (1973); *Phys. Rev.* **D10**, 275 (1974).
[29] UA1 Collaboration, G. Arnison et al., *Phys. Lett.* **122B**, 103 (1983); *Phys. Lett.* **126B**, 398 (1983). UA2 Collaboration, M. Banner et al., *Phys. Lett.* **122B**, 476 (1983); *Phys. Lett.* **129B**, 130 (1983).
[30] S. Weinberg, *Phys. Rev.* **D7**, 1888 (1976); L. Susskind, *Phys. Rev.* **D20**, 2615 (1979); E. Fahri, L. Susskind, *Phys. Rep.* **74C**, 277 (1981).
[31] For a review see for example: M. E. Peskin, Proceedings of the 1981 International Symposium on Lepton and Photon Interactions at High Energies, Bonn, August 1981.
[32] P. Fayet, S. Ferrara, *Phys. Rev.* **32C**, 249 (1977).
[33] S. Rudaz, J. Vermaseren, CERN Preprint TH-2961 (1981).
[34] R. Rückel, MPI — PAE/PTH 24/83 and 35/83.
[35] S. K. Jones, C. H. Llewellyn-Smith, *Nucl. Phys.* **B217**, 145 (1983).
[36] P. Salati, J. C. Wallet, LAPP-TH-65 (1982).